Supplementary Materials

Text S1.

1. Supplementary Methods

To assess the environmental drivers of the interannual variability in mature female krill condition during the spawning season from 1993-2008 at the western Antarctic Peninsula (wAP), we ran generalized additive models (GAMs) using the 'mgcv' package in RStudio (v. 1.3.959) (Wood 2011, RStudio Team 2020). We examined seasonal phases for the Southern Annular Mode (SAM) and the Multivariate El Niño Oscillation Index (MEI) as potential climatological drivers of mature female krill condition. Oceanographic variables that we considered as potential predictors of mature female krill condition included: sea surface temperature (SST), depth of the winter water layer (WWL), depth of the surface mixed layer (SML), the water stratification index, and the anomalies of the day of sea ice advance, day of sea ice retreat and sea ice season duration. Integrated chlorophyll-*a* (Chl-*a*), a proxy for phytoplankton biomass (Garibotti et al. 2003), integrated fucoxanthin, a proxy for diatom biomass (Kavanaugh et al. 2015), and the proportion of integrated fucoxanthin to Chl-*a* were also predictor variables of interest due to their established correlation with krill abundances (Steinberg et al. 2015). Below we discuss environmental data collection and our statistical modelling protocols in more detail.

1.1 Climate indices

We examined seasonal phases for SAM and MEI as potential drivers of mature female krill condition during the spawning season. Monthly SAM data were obtained from the online database established by the Natural Environmental Research Council (NERC) British Antarctic Survey (BAS) (http://www.nerc-bas.ac.uk/icd/gima/sam/html; Marshall 2003). Monthly MEI data were obtained from the National Oceanic and Atmospheric Administration (NOAA), Earth System Research Laboratory (ESRL), Physical Sciences Division (http://www.esrl.noaa.gov/psd/ data/ correlation/mei.data; Wolter & Timlin 2011). Seasonal SAM and MEI were calculated based on the average values observed during the austral autumn (March-May), winter (June-August) and spring (September-November) for the years 1992-2007 to correspond with the summers of 1993-2008, and during the summer (December-February) where values from December the prior year were averaged with those from January and February in the year of each survey (e.g. December 1992 with January and February 1993 to correspond with mature female krill condition during the summer of 1993).

1.2 Oceanographic and Phytoplankton Biomass parameters

Oceanographic variables that we considered as potential predictors of mature female krill condition included: SST, depth of the WWL, depth of the SML, the water stratification index, and the anomalies of the day of sea ice advance, day of sea ice retreat and sea ice season duration. Integrated Chl-*a,* a proxy for phytoplankton biomass (Garibotti et al. 2003), integrated fucoxanthin, a proxy for diatom biomass (Kavanaugh et al. 2015), and the proportion of integrated fucoxanthin to Chl-*a* were predictor variables of interest due to their established correlation with krill abundances (Steinberg et al. 2015). A Seabird 911 was used to collect SST, CTD, Chl-*a* and fucoxanthin data at the same sampling stations where krill were collected. Sea ice data were calculated based on satellite observations of sea ice concentrations. The depth of the WWL and

SML and the water stratification index were calculated using CTD data. All environmental data were obtained from the PAL LTER Datazoo online database: https://oceaninformatics.ucsd.edu/datazoo/catalogs/pallter/datasets.

SST data were obtained from CTD casts and seawater samples at each station. After every cruise, temperature and conductivity sensors were calibrated and post-cruise processing was applied. In addition to the pre-cruise calibration of the CTD, post-cruise calibration and SeaBird software and algorithms were used to obtain the highest quality CTD data. Each profile is inspected for issues and the sensors are calibrated as needed (Iannuzzi 2018). The temperature minimum (T_{min}) identified the depth of the remnant WWL. The depth of the SML was defined as the depth where the density gradient from the surface reached 0.125 (Levitus 1982). We calculated the density at the surface (sigma-theta$_{surf}$; kg m^{-3}) and at the depth of the temperature minimum (sigma-theta$_{Tmin}$), for each CTD cast. We then calculated the depth at which the surface temperature was recorded (D_{Tsurf}), the density at the temperature minimum (sigma-theta$_{Tmin}$), and the depth at which the temperature minimum was recorded (D_{Tmin}) for each CTD cast. The water stratification index was: Strat = (sigma-theta $_{Tmin}$ − sigma-theta$_{Tsurf}$)/(D_{Tmin} D_{Tsurf}) where D_{Tmin} is the depth of the temperature minimum (Saba et al. 2014). Values for the stratification index fell between 0 and 0.1, with values closer to 0.1 signifying a greater stratification of the water column.

The annual timing of sea ice advance and retreat, and sea ice season duration were derived for the PAL LTER region using passive microwave satellite data. Sea ice extent was first determined using Near-Real-Time-Sea-Ice (NRTSI) data, then an area mean was calculated for the Palmer Basin Region using the version 2 of the Bootstrap algorithm derived by Goddard Space Flight Center (Stammerjohn 2020). The sea ice season duration was defined as the time elapsed between the day of ice advance and the day of ice retreat within a given sea ice year (mid-February to the following mid-February) (Stammerjohn et al. 2008a). Sea ice parameters were calculated separately for the northern and southern wAP. The area used to calculate sea ice indices at the northern wAP spanned ~200 km west and south of Anvers Island (i.e. 400-600 grid-lines) and, at the southern wAP ~200 km west and south of Avian Island which is a small island located at the southern tip of Adelaide Island (i.e. 200-300 grid-lines). Annual anomalies for the day of sea ice advance and retreat and for sea ice duration were calculated for both regions for each year between 1993 and 2008 using mean values for the full period of the sea ice satellite record, 1978-2019.

Seawater samples for Chl-*a* and fucoxanthin were collected at various depths in the water column with Niskin bottles during CTD casts, and at the surface with the ship's flow-through seawater system. The depths for Chl-*a* sample collection were chosen based on the depths of the 1, 5, 10, 30, 60, and 100% light levels. Chl-*a* concentrations were determined from seawater samples filtered onto GF/F filters, frozen at -80°C, and analyzed immediately after the cruise at Palmer Station (Schofield et al. 2020). Concentrations of fucoxanthin and other accessory pigments were measured using high performance liquid chromatography (HPLC). HPLC samples were collected from the same CTD casts as the Chl-*a* samples. After filtering the seawater onto GF/F filters and freezing them at 80˚C, HPLC analysis was carried out following the procedure outlined by Wright et al. (1991). Following the guidelines developed by the NASA SeaWiFS HPLC Analysis Round-Robin Experiment (SeaHARRE), an internal standard was used along with replicate injects on the HPLC to track recovery and replicability of the pigment extraction methods and the HPLC (Schofield et al. 2018). HPLC data were not available for the PAL LTER summer cruises in 2002 and 2005. For each sampling station, the depth-integrated Chl-*a* and fucoxanthin concentrations (mg m^{-2}) were calculated for the top 200 m of the water column. Although krill were only collected within the top 120 m of the water column, they will vertically migrate to depths below

the euphotic zone (which is variable, but at an average of 200 m depth) to forage for phytoplankton (Steinberg & Landry 2017). For this reason, we chose to integrate Chl-*a* and fucoxanthin concentrations over the top 200 m to reflect the available food for grazing krill. The proportion of integrated fucoxanthin to Chl-*a* was also determined to ascertain how much primary productivity in the water was due to diatoms.

1.3 Statistical analyses for the environmental drivers of variability in mature female krill condition during the spawning season at the wAP

The number of potential predictor variables (n=18) was large, which negatively affects the efficacy of GAMs. Thus, we first grouped the potential predictor variables into three categories (Climatological, Oceanographic, and Phytoplankton Biomass) and ran separate GAMs using the set of variables within each category (Table S1). In this way, we identified the climatological, oceanographic and phytoplankton biomass predictor variables that had the strongest effects on mature female krill condition during the spawning season.

Prior to running our Climatological, Oceanographic, and Phytoplankton Biomass models, variance inflation factors (VIF) were estimated to check for violations in collinearity. The variance of the regression coefficient estimates is inflated when there is correlation among the predictor variables. For each covariate, the recommendation is to restrict the VIF to a value no greater than 3 (Zuur et al. 2010), which is the VIF threshold that was applied to these models. Due to collinearity restrictions, not all of the potential predictor variables could be included in the same model, therefore several iterations of the Climatological, Oceanographic and Phytoplankton Biomass Models were run ensuring that each of the potential predictor variables for each model was included in at least one iteration. Each GAM was formulated with mature female krill condition during the spawning season as the response variable and incorporated a fixed spatial factor separating the data collected from the northern and southern wAP. A gamma value of 2 was incorporated into each model, putting extra penalty on the roughness of the model and ensuring that the proper relationships between each covariate and mature female krill condition were identified (Wood et al. 2016). If the smoothing term of a covariate was not statistically significant ($p > 0.05$), it was removed from the model. This process was repeated for each non-significant smoothing term until all covariates in the model had a significant relationship with mature female krill condition. Modelling analyses were conducted using a Gaussian error distribution, and the GAMs with a low Akaike Information Criterion (AIC) score and those that had the smallest minimized generalized cross-validation (GCV) score were selected as the best models. AIC measures the goodness of a model fit and the model with the lowest AIC is considered the best model based on the model fit and complexity (Bozdogan 1987). Low GCV scores indicate a lower prediction error and a better fitting model (Zuur et al 2009).

VIFs were once again calculated prior to running the Full Model. Covariates from the Phytoplankton Biomass Model (integrated Chl-*a*, integrated fucoxanthin and the proportion of integrated fucoxanthin to Chl-*a*) were not considered for the Full Model because, unlike the covariates in the Climatological and Oceanographic Models, they did not contain data from 2002 and 2005. None of the covariates from the best Climatological and Oceanographic Models had VIFs > 3 when grouped together, therefore all covariates were included in the Full Model. After removing the non-significant smoothing terms, model comparisons were carried out using AIC and GCV scores. Residual validations followed to ensure that each model met the GAM assumptions of normality, homogeneity of variance and independence.

SAM and MEI can have amplifying effects during the same season when in opposing phases at the wAP (Stammerjohn et al. 2008b). Because of this, we constructed an interactive model for spring SAM and MEI with a fixed spatial factor separating the data between the northern and southern wAP. We ran an interactive model for the spring climate variables because it was the only season where both SAM and MEI were shown to be significantly correlated with mature female krill condition during the spawning season. We then compared this model to an additive model to see which performed better. AIC and GCV scores were used for model comparison, however because GCV scores do not properly account for the threshold parameter that we used in the interactive model (Ciannelli et al. 2004), we also performed a genuine cross validation (gCV) on both models to ensure that we identified the best model. The gCV was calibrated with 500 model iterations of the dataset. For each model iteration, a random selection of 20 data points (~8% of the entire dataset) was excluded from the model calibration and the resulting 237 data points (~92% of the entire dataset) were used to predict the data not included in the model. The final cross validation of the model was calculated as the mean of mean-squared predictive error from each iteration. Similar to GCV scores, low gCV scores indicated a better model fit. The additive model performed better than the interactive model, therefore we used the results from the additive models for spring SAM and MEI.

TEXT S2.

2 Supplementary Results

2.1 The timing of sea ice advance and retreat, and integrated fucoxanthin concentration as regional drivers of mature female krill condition during the spawning season at the wAP

Prior to combining predictor variables in the Full Model, results from the Oceanographic Model suggested that the anomalies of the day of sea ice advance and retreat were drivers of mature female krill condition during the spawning season at the wAP from 1993-2008 (Table 1 in the main article; see also Supplementary Table S1). The timing of sea ice advance and retreat were positively correlated with mature female krill condition during the spawning season (Fig. S1) and explained 17% of the deviance in the Oceanographic Model (Supplementary Table S1). Mature female krill condition during the spawning season was highest when sea ice advanced at least 20 days later than average and lowest when sea ice retreated at least 40 days earlier than average. Prior to combining predictor variables in the Reduced Model, results of the Phytoplankton Biomass Model identified integrated fucoxanthin concentration, a proxy for diatom biomass, as a driver of mature female krill condition during the spawning season at the wAP from 1993-2008 (Table 1 in the main article, see also Supplementary Table S1). However, the relationship was weak (Fig. S2) and only accounted for 5.3% of the deviance explained in the Phytoplankton Biomass Model (Supplementary Table S1). While sea ice advance and sea ice retreat were significant predictor variables in the Oceanographic Model, they were not significant when combined with the climate predictor variables in the Full Model (Table 2 in the main article, see also Supplementary Table S2). Similarly, when the integrated fucoxanthin concentration was combined with the other predictor variables in the Reduced Model, it was not a significant driver of mature female krill condition (Table 2 in the main article, see also Supplementary Table S2).

References

Bozdogan H (1987) Model selection and Akaike's Information Criterion (AIC): The general theory and its analytical extensions. Psychometrika 52:345–370 doi:10.1007/BF02294361

Ciannelli L, Chan KS, Bailey KM, Stenseth NC (2004) Nonadditive Effects of the Environment on the Survival of a Large Marine Fish Population. Ecology 85:3418–3427 doi:10.1890/03-0755

Garibotti IA, Vernet M, Kozlowski WA, Ferrario ME (2003) Composition and biomass of phytoplankton assemblages in coastal Antarctic waters: a comparison of chemotaxonomic and microscopic analyses. Mar Ecol Prog Ser 247:27–42 doi:10.3354/meps247027

Iannuzzi R. (2018) Conductivity Temperature Depth (CTD) sensor profile data binned by depth from PAL LTER annual cruises, 1991 - 2017 (ongoing). ver 2. Environmental Data Initiative

Kavanaugh MT, Abdala FN, Ducklow HW, Glover D and others (2015) Effect of continental shelf canyons on phytoplankton biomass and community composition along the western Antarctic Peninsula. Mar Ecol Prog Ser 524:11–26 doi:10.3354/meps11189

Levitus S (1982) Climatological Atlas of the World Ocean. U.S. Department of Commerce, National Oceanic and Atmospheric Administration.

Marshall GJ (2003) Trends in the Southern Annular Mode from Observations and Reanalyses. J Clim 16:4134–4143 doi:10.1175/1520-0442(2003)016<4134:TITSAM>2.0.CO;2

RStudio Team (2020) RStudio: Integrated Development Environment for R. RStudio, PBC, Boston, MA.

Saba GK, Fraser WR, Saba VS, Iannuzzi RA and others (2014) Winter and spring controls on the summer food web of the coastal West Antarctic Peninsula. Nat Commun 5:. art4318PubMed

Schofield O, Vernet M, Prezelin B (2018) Photosynthetic pigments of water column samples and analyzed with High Performance Liquid Chromatography (HPLC), collected aboard Palmer LTER annual cruises off the coast of the Western Antarctica Peninsula, 1991 – 2016 (ongoing). Environmental Data Initiative.

Schofield O, Vernet M, Smith R (2020) Chlorophyll and phaeopigments from water column samples, collected at selected depths aboard Palmer LTER annual cruises off the coast of the Western Antarctic Peninsula, 1991 – 2019 (ongoing). Environmental Data Initiative.

Stammerjohn S (2020) Sea ice duration or the time elapse between day of advance and day of retreat within a given sea ice year for the PAL LTER region West of the Antarctic Peninsula derived from passive microwave satellite, 1978 – 2019 (ongoing). Environmental Data Initiative.

Stammerjohn SE, Martinson DG, Smith RC, Iannuzzi RA (2008a) Sea ice in the western Antarctic Peninsula region: Spatio-temporal variability from ecological and climate change perspectives. Deep Sea Res II 55:2041–2058 doi:10.1016/j.dsr2.2008.04.026

Stammerjohn SE, Martinson DG, Smith RC, Yuan X, Rind D (2008b) Trends in Antarctic annual sea ice retreat and advance and their relation to El Niño–Southern Oscillation and Southern Annular Mode variability. J Geophys Res 113:3

Steinberg DK, Landry MR (2017) Zooplankton and the Ocean Carbon Cycle. Annu Rev Mar Sci 9:413–444 PubMed doi:10.1146/annurev-marine-010814-015924

Steinberg DK, Ruck KE, Gleiber MR, Garzio LM and others (2015) Long-term (1993–2013) changes in macrozooplankton off the Western Antarctic Peninsula. Deep Sea Res I Oceanogr Res Pap 101:54–70 doi:10.1016/j.dsr.2015.02.009

Wolter K, Timlin MS (2011) El Niño/Southern Oscillation behaviour since 1871 as diagnosed in an extended multivariate ENSO index (MEI.ext). Int J Climatol 31:1074–1087 doi:10.1002/joc.2336

Wood SN (2011) Fast stable restricted maximum likelihood and marginal likelihood estimation of semiparametric generalized linear models. J R Stat Soc Series B Stat Methodol 73:3–36 doi:10.1111/j.1467-9868.2010.00749.x

Wood SN, Pya N, Säfken B (2016) Smoothing Parameter and Model Selection for General Smooth Models. J Am Stat Assoc 111:1548–1563 doi:10.1080/01621459.2016.1180986

Wright SW, Jeffrey SW, Mantoura RFC, Llewellyn CA, Bjornland T, Repeta D, Welschmeyer N (1991) Improved HPLC method for the analysis of chlorophylls and carotenoids from marine phytoplankton. Mar Ecol Prog Ser 77:183–196 doi:10.3354/meps077183

Zuur AF, Ieno EN, Walker N, Saveliev AA, Smith GM (2009) Mixed effects models and extensions in ecology with R. Springer New York, NY.

Zuur AF, Ieno EN, Elphick CS (2010) A protocol for data exploration to avoid common statistical problems: Data exploration. Methods Ecol Evol 1:3–14 doi:10.1111/j.2041-210X.2009.00001.x

3 Supplementary Figures

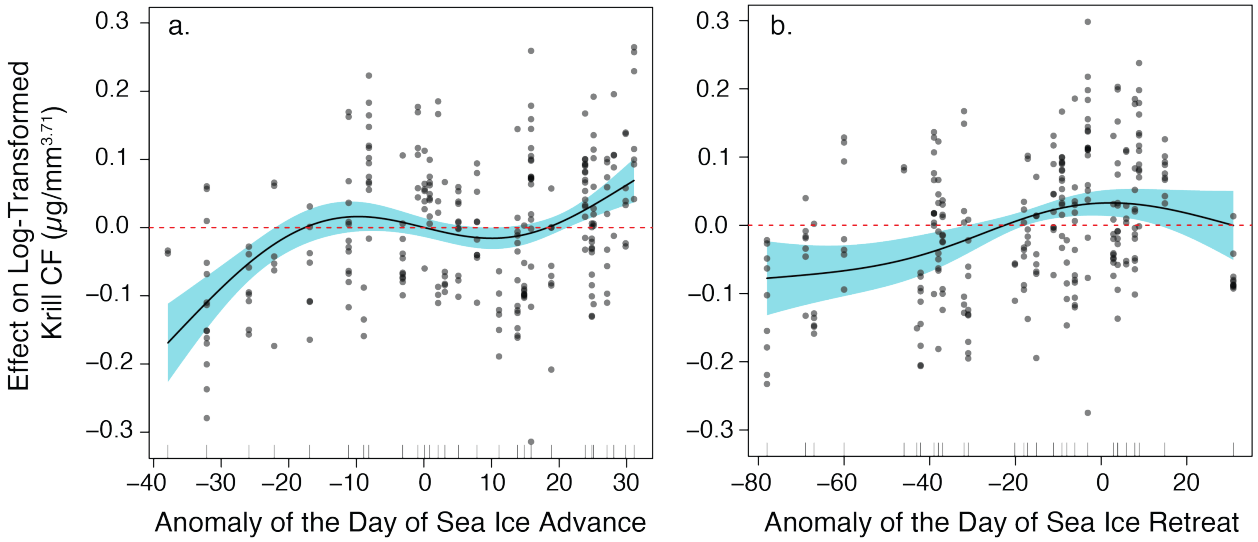

Figure S1. The relationship between the anomaly of mature female krill condition factor (CF; µg $mm^{-3.71}$) during the spawning season and a) the anomaly of the day of sea ice advance and b) the anomaly of the day of sea ice retreat at the western Antarctic Peninsula (wAP) from 1993-2008 as determined by the best performing Oceanographic GAM. The red dashed line represents a zero anomaly and the points are the model residuals.

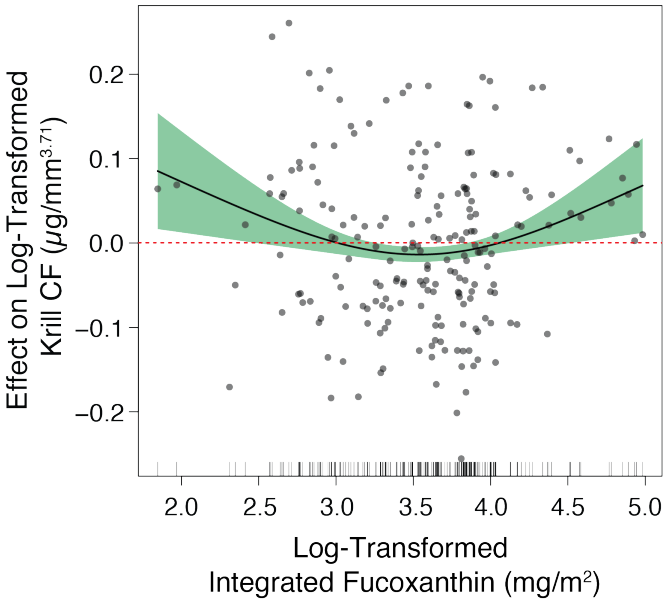

Figure S2. The relationship between the anomaly of mature female krill condition factor (CF; µg $mm^{-3.71}$) during the spawning season and integrated fucoxanthin (mg m^{-2}) at the western Antarctic Peninsula (wAP) from 1993-2008 as determined by the best performing Phytoplankton Biomass GAM. The red dashed line represents a zero anomaly and the points are the model residuals.

4 Supplementary Tables

Table S1. The models used to identify 1) the relationships between mature female krill condition factor (CF; µg $mm^{-3.71}$) during the spawning season and climatological variability at the Western Antarctic Peninsula (wAP) from 1993-2008, 2) the relationships between mature female krill CF during the spawning season and sea ice variability at the wAP from 1993-2008, and 3) the relationship between mature female krill CF during the spawning season and integrated fucoxanthin at the wAP from 1993-2008. The model formulations expressed below only show the covariates that were significantly correlated with mature female krill condition during the spawning season. The (*) is used to denote which models performed the best. Abbreviations in the formulations: CF = log-transformed mature female krill CF during the spawning season, NS = north/south, SAMAUT = autumn SAM index, SAMWIN = winter SAM index, SAMSPR = spring SAM index, SAMSUM = summer SAM index, MEIAUT = autumn MEI index, MEIWIN = winter MEI index, MEISPR = spring MEI index, MEISUM = summer MEI index, IceAdv = anomaly of the day of ice advance, IceRet = anomaly of the day of ice retreat, IceDur = anomaly of the sea ice season duration, and logFuc = log-transformed integrated fucoxanthin concentration (mg m^{-2}). AIC is the Akaike Information Criterion score, GCV is the Generalized Cross-Validation score, R^2 is the value that represents the fit of the data to the regression line, and Dev. Exp. is the percentage of deviance explained by the model.

Model	Iteration	Formulation	AIC	GCV	R^2	Dev. Exp. (%)
1. Climatological GAM	1	*CF ~ factor(NS) + s(SAMWIN, k = 3) + s(SAMSPR, k = 4) + s(SAMSUM, k = 3) + s(MEIAUT, k = 3)+ s(MEIWIN, k = 3)*	522.32	-.008	.287	1.0
	2	*CF ~ factor(NS) + s(SAMAUT, k = 3) + s(SAMSPR, k = 4) + s(SAMSUM, k = 3) + s(MEIWIN, k = 3)*	527.92	-.008	.302	2.4
	3	*CF ~ factor(NS) + s(SAMAUT, k = 3) + s(SAMSPR, k = 4) + s(SAMWIN, k = 3) + s(MEIWIN, k = 3)*	551.80	-.007	.362	8.0
	4	*CF ~ factor(NS) + s(SAMWIN, k = 3) + s(SAMSPR, k = 4) + s(SAMSUM, k = 3) + s(MEIAUT, k = 3)*	515.56	-.008	.263	8.3

	5	*CF ~ factor(NS) + s(SAMWIN, k = 3) + s(SAMAUT, k = 3) + s(SAMSUM, k = 3) + s(MEISUM, k = 3)*	517.33	- .008	.268	8.7
	6	*CF ~ factor(NS) + s(SAMWIN, k = 3) + s(SAMSPR, k = 4) + s(SAMAUT, k = 3) + s(MEISUM, k = 3)*	549.25	- .007	.355	7.4
	7	*CF ~ factor(NS) + s(SAMWIN, k = 3) + s(SAMSPR, k = 4) + s(SAMAUT, k = 3) + s(SAMSUM, k = 3) + s(MEISUM, k = 3)*	559.62	- .007	.386	0.8
	8*	*CF ~ factor(NS) + s(SAMAUT, k = 3) + s(SAMWIN, k = 3) s(SAMSPR, k = 4) + s(SAMSUM, k = 3) + s(MEISPR, k = 3)*	564.38	- .007	.397	2.0
2. Oceanographic GAM	1*	*CF ~ factor(NS) + s(IceAdv, k = 4) + s(IceRet, k = 4)*	478.69	- .010	.148	7.0
	2	*CF ~ factor(NS) + s(IceDur, k = 4) + s(IceRet, k = 4)*	464.89	- .010	.092	0.6
3. Phytoplankton Biomass GAM	1*	*CF ~ factor(NS) + s(logFuc, k = 3)*	417.33	- .009	.043	.48

Table S2. The models used to identify 1) the relationships between mature female krill condition factor (CF; µg $mm^{-3.71}$) during the spawning season and predictor variables included in the Full Model and 2) the relationships between mature female krill CF during the spawning season and predictor variables included in the Reduced Model at the Western Antarctic Peninsula (wAP) from 1993-2008. The model formulations expressed below only show the covariates that were significantly correlated with mature female krill condition during the spawning season. The (*) is used to denote which models performed the best. Abbreviations in the formulations: CF = log-transformed mature female krill CF during the spawning season, NS = north/south, SAMAUT = autumn SAM index, SAMWIN = winter SAM index, SAMSPR = spring SAM index, SAMSUM = summer SAM index, MEISPR = spring MEI index, MEISUM = summer MEI index, IceAdv = anomaly of the day of ice advance and IceRet = anomaly of the day of ice retreat. AIC is the Akaike Information Criterion score, GCV is the Generalized Cross-Validation score, R^2 is the value that represents the fit of the data to the regression line, and Dev. Exp. is the percentage of deviance explained by the model.

Model	Iteration	Formulation	AIC	GCV	R^2	Dev. Exp. (%)
1. Full GAM	1*	*CF ~ factor(NS) + s(SAMAUT, k = 3) + s(SAMWIN, k = 3) + s(SAMSPR, k = 4) + s(SAMSUM, k = 3) + s(MEISPR, k = 3)+*	-564.38	.007	.397	42.0
	1	*CF ~ factor(NS) + s(IceAdv, k = 4) + s(IceRet, k = 4) + s(SAMWIN, k = 3) + s(SAMSPR, k = 4)*	-384.46	.007	.309	33.4
2. Reduced GAM	2*	*CF ~ factor(NS) + s(IceAdv, k = 4) + s(IceRet, k = 4) + s(SAMAUT, k = 3) + s(SAMWIN, k = 3)*	-388.17	.007	.310	33.4
	3	*CF ~ factor(NS) + s(IceRet, k = 4) + s(SAMAUT, k = 3) + s(SAMWIN, k = 3) + s(SAMSUM, k = 3)*	-383.96	.008	.292	31.4

Table S3. The average mature female krill condition factor during the spawning season (CF; µg $mm^{-3.71}$) and the average number of eggs per mature female krill at the wAP from 1993-2008.

Year	Mature Female CF	Egg Batch Size
1993	0.58	2339
1994	0.57	2565
1995	0.65	5419
1996	0.66	5948
1997	0.60	2158
1998	N/A	2672
1999	0.55	3251
2000	0.65	3010
2001	0.64	6069
2002	0.66	5693
2003	0.55	N/A
2004	0.58	2076
2005	0.55	3421
2006	0.60	5299
2007	0.58	4094
2008	0.56	4329